Structure and Morphology of Odd Polyoxamides [Nylon 9,2]. A New Example of Hydrogen-Bonding Interactions in Two Different Directions

L. Franco, J. A. Subirana, and J. Puiggalí*

Departament d'Enginyeria Química, ETS d'Enginyers Industrials, Universitat Politècnica de Catalunya, Diagonal 647, Barcelona 08028, Spain

Received October 30, 1997; Revised Manuscript Received February 26, 1998

ABSTRACT: The structure and morphology of nylon 9,2 has been investigated using transmission electron microscopy, selected area electron diffraction, and X-ray diffraction. A unit cell with parameters a = 5.45 Å, b = 8.7 Å, c (chain axis) = 31.8 Å, and β = 47.9° was determined and a $C12/c1$ space group is postulated. Chain conformation is practically all-trans, but the torsion angles of the $NH-CH_2$ bonds slightly deviate from 180° in order to optimize the hydrogen-bonding interactions between neighboring chains. A structure with two directions of hydrogen bonding is derived, although the unit cell is strongly related to that found in nylon 6,6. Crystallization from the melt and temperature-induced structural changes have also been studied.

Introduction

Different articles and patents on polyoxamides have been reported,[1−9] since they present some interesting properties such as (a) high melting temperatures, (b) low solubility, and (c) a high modulus. Many of these works indicate thermal instability during the preparation and processing of polyoxamides, so their commercial applications appear to be limited. However, accurate thermal gravimetric analysis[10] of some polymers have demonstrated that decomposition takes mostly place in the 400−475 °C interval and takes place preferentially when the oxamide/methylene ratio is high. Thus, the limited thermal stability is similar to conventional polyamides and it is not a deterrent for applications. On the other hand, valuable characteristics have been reported in regular copolymers based on the oxamide linkage, as for example in desalination membranes.[11]

Polyoxamides of reasonable molecular weight cannot be easily prepared by the normal polymerization techniques used for polyamides. Thus, the melt polycondensation route of Carothers from a diamineoxalate is not possible due to thermal decomposition of both the oxalic acid[12] and the polymer. Similarly, a slow thermal decomposition is also observed in the preparation by ring opening of cyclic oxamides.[13] The standard liquid−liquid interfacial polymerization has also not been useful because of rapid hydrolysis of the diacid chloride. However, fiber-forming polyoxamides[14] can be prepared by a gas−liquid interfacial polymerization technique in which oxalyl chloride is bubled into an aqueous solution of the diamine. High molecular weight can also be achieved by a two-stage procedure where first a prepolymer is formed at low temperature from a diester of oxalic acid and a diamine and then a postpolymerization is carried out at higher temperatures (250−300 °C).[10,15]

All the published structural data on polyoxamides refer to the even diamine derivatives and only correspond to X-ray diffraction studies. Thus, powder patterns have been reported for nylons 10,2,[10] 8,2,[10] 6,2,[10] and 4,2,[15] whereas fiber patterns have only been reported for nylons 6,2[14] and 12,2.[10] In general the number of observed reflections is small, and in fact the unit cell parameters could only be approximately determined for nylon 6,2.[14] An extended planar zigzag conformation for the polyoxamide chains has been proposed in all cases, with intermolecular hydrogen bonds between neighboring molecular chains, as shown in Figure 1a. The oxamide part of the zigzag is assumed to be unusually stiff by virtue of the quasi-conjugated prototropic systems constituting the coplanar structure. The structure proposed for nylon 6,2[14] indicates a shift between neighboring hydrogen-bonded sheets, in a way similar to the characteristic α-form of nylons.[16]

In nylons, another structure based on a not-extended conformation and named the γ-form[16,17] is found when the methylene/amide ratio is high (for nylons n) or when hydrogen bonds cannot be well established with the extended conformation, as it happens with nylons m,n [$-(NH(CH_2)_mNHCO(CH_2)_{n-2}CO)_x-$] when m and/or n are odd. Both structures can be well differentiated by diffraction data since (a) the γ-form presents a characteristic shortening of the chain repeat unit of about 0.35 Å/amide group and (b) chain packing changes from the triclinic/monoclinic one characteristic of the α-form (with diffraction spacings at 4.40 and 3.80 Å) to hexagonal (or very close to hexagonal) with a single spacing at 4.15 Å. Although a single hydrogen bond direction is usually postulated for both structures, different models with three or two directions have also been reported for polymers quenched from the melt[18] and for nylon 8 fibers,[19] respectively. Recently, we have also reported structures with two hydrogen bond directions for nylons m,n derived from malonic and glutaric acids (n odd), taking into account data from fibers and chain-folded lamellar crystals of polymers,[20−23] as well as from model compounds.[24−26]

In this sense, odd polyoxamides constitute an interesting system, since (a) only one kind of methylene segment exists in contrast to the previously indicated nylons m,n and (b) the extended conformation found in even polyoxamides seems to be unfavorable because of hydrogen bonds cannot be well established (Figure 1b). The aim of this work is to report structural data (X-ray and electron diffraction) of a representative odd polyoxamide. Nylon 9,2 has been selected due to the relatively high methylene/oxamide ratio (similar to the equivalent methylene/amide ratio of nylon 6,6) which increases its thermal stability. To obtain fiber X-ray

S0024-9297(97)01599-4 CCC: $15.00
Published on Web 05/23/1998

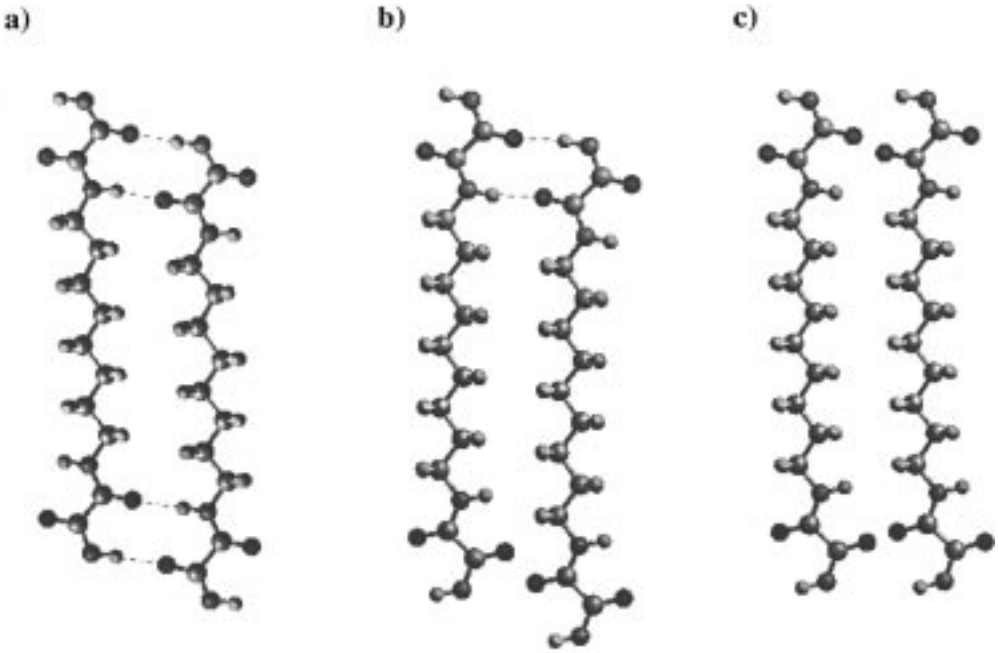

Figure 1. All-trans conformation postulated for even polyoxamides. As illustrated in part a for nylon 8,2, hydrogen bonds (indicated by dashed lines) with optimum geometry can be established between neighboring chains when they are shifted. In odd polyoxamides with an extended conformation only 50% of hydrogen bonds can be established between neighboring chains as shown in part b. This fact is a consequence of the opposite relative orientation of consecutive oxamide groups along the polymer chain. When the neighboring molecular chains are not shifted, the NH and CO groups are too far away to produce hydrogen-bonding interactions. Furthermore, strong repulsive interactions appear because of carbonylic groups face up as illustrated in part c.

diffraction data, a special attention has been given to the synthesis of polymers with appropriate molecular weights.

Experimental Section

Synthesis and Characterization. Nylon 9,2 was prepared from 1,9-diaminononane and diethyl oxalate according to the two step synthesis reported by Shalaby et al.[10] Diethyl oxalate was distilled prior to use, whereas other reagents and solvents (ACS grade) were used as received.

The stoichiometric amount of diethyl oxalate was added to a stirred solution of 1,9-diaminononane in trifluoroethanol (concentration 10% w/v). After 20 min at room temperature, the reaction mixture was refluxed (80 °C) for 5 h. The prepolymer gradually precipitated from solution. However after the indicated time, the solution was cooled and petroleum ether was added in order to recover the most soluble oligomers. The product was washed only with ethanol and dried in a vacuum oven. Water contact was avoided during washing and storing, since it has been demonstrated[15] that hydrolysis of the terminal ester groups strongly decreases the molecular weight of post-polycondensate samples.

The prepolymer was post-polymerized in small tubes under a stream of dry nitrogen or under vacuum. Different polycondensations were done varying time (from 40 to 420 min), whereas the temperature was kept close to 250 °C (by using a silicone−oil bath) in order to minimize decomposition and to keep the polymer in the melt state. Post-polycondensed samples were purified by precipitation with water of dichloroacetic acid solutions (1% w/v) and then successively washed with water, ethanol, and ethyl ether.

The intrinsic viscosity of the polymer was determined by measurements with a Cannon-Ubbelohde microviscometer in dichloroacetic acid solutions at 25 ± 0.1 °C. The density of the powder sample was measured at 25 °C by the flotation method in mixtures of ethanol and carbon tetrachloride. The chemical constitution of the polymer was ascertained by infrared and NMR spectroscopy and elemental analysis. The infrared absorption spectrum was recorded from potassium bromide pellets with a Perkin-Elmer 1600 FT-IR spectrophotometer in the 4000−500 cm^{-1} range. NMR spectra were registered from polymer solutions in deuterated trifluoroacetic acid using a Bruker AMX-300 spectrometer operating at 300.1 MHz for ^1H NMR and at 75.5 MHz for ^{13}C NMR.

Thermal behavior was investigated with a Perkin-Elmer DSC-4 equipped with a TADS data station at a heating rate of 20 °C/min in a nitrogen atmosphere. The instrument was calibrated for temperature (T) and heat of fusion (ΔH) using an indium standard ($T_m = 429.5$ K, $\Delta H_m = 3.267$ kJ/mol). The expected accuracy is 1−2 K for T and ±3% for ΔH. A baseline was always run and subtracted to avoid the effects of the changing environment.

Structural Methods. Spherulites were grown from melt-crystallized thin films which were produced by heating small amounts of polymer on microscope slides. When the polymer was molten, films were pressed or smeared between cover slips and the slides. The films were crystallized isothermally at different temperatures below the melting point, using a Mettler FP80 thermal analysis system instrument. At the end of the crystallization periods the films were quenched in solid CO_2−acetone in order to arrest the crystallization. Morphologies of melt-grown spherulites were observed by polarizing optical microscopes (Nikon Microflex AFX-DX and Carl Zeiss Standard GFL). Photographs were taken using the Nikon microscope equipped with a Nikon FX-35DX camera. A first-order red tint plate was used to determine the sign of spherulite birefringence under cross-polarization.

Crystallization experiments were also carried out isothermally from dilute 1,4-butanediol solutions (0.05−0.1% (w/v)). The crystals were recovered from mother solutions by centrifugation and were repeatedly washed with *n*-butanol.

For electron microscopy the crystals were deposited on carbon-coated grids which were then shadowed with Pt−carbon at an angle of 15°. The crystals were also decorated with polyethylene vapors before shadowing. A Philips EM-301 electron microscope operating at either 80 or 100 kV for bright field and electron diffraction modes, respectively, was used throughout this work. Electron diffraction diagrams were recorded by the selected area method on Kodak Tri-X films. The patterns were internally calibrated with gold ($d_{111} = 2.35$ Å).

X-ray diagrams were recorded under vacuum at room temperature, and calcite (d_B= 3.035 Å) was used for calibration. A modified Statton camera (W. R. Warhus, Wilmington, DE) with Ni-filtered Cu Kα radiation of wavelength 1.542 Å was used for these experiments. Patterns were recorded from either polymer powders, fibers, or mats of single crystals which were prepared by slow filtration of a crystal suspension on a glass filter. X-ray diagrams were also recorded as a function of temperature by using a temperature-controlled chamber provided by the manufacturer.

Structural modeling was carried out by using the software package CERIUS 3.1 (Biosym/Molecular Simulations Inc.). Peaks in the simulated fiber diffraction patterns were broadened with a Lorentzian profile, and a disorientation angle was introduced in order to reproduce the arched reflections. Polarization and temperature factors were included in calculations that were run on a Silicon Graphics Indigo Workstation.

Results and Discussion

Synthesis and Characterization. The solution polymerization of diethyloxalate gave a prepolymer with 70% yield and an intrinsic viscosity of 0.10 dL/g. Signals attributed to both kind of terminal groups (ethyl ester and diamine) were observed in the NMR spectra, and so a thermal post-polymerization was carried out.

An intrinsic viscosity around 0.25 dL/g, independent of the polymerization time in the 40−210 min interval, was found when post-polymerization was conducted under a nitrogen atmosphere. This value suggests equilibrium between polymerization and decomposition rates. In fact, it is well-known that the limited thermal stability of polyoxamides has been a major problem in obtaining high molecular weight polymers.[27] However, when the polymerizations were carried out under vacuum the intrinsic viscosity increased with polymerization time, because of the increasing polymerization rate. Thus, values of 0.38, 0.57, and 0.97 dL/g were respectively obtained for 90, 240, and 420 min post-polymerized samples, respectively. All of them showed a slightly brown coloration indicative of some degradative reactions. Samples with an intrinsic viscosity equal or higher than 0.57 dL/g had fiber-forming properties. In all cases a yield around 60% was found after precipitation from dichloroacetic acid solutions.

The chemical shifts of the intense signals observed in both ^{1}H and ^{13}C NMR spectra are in full agreement with the anticipated chemical composition. ^{1}H NMR (300.1 MHz, TFA-*d*): δ 3.46 (4H, t, α-methylene), 1.71 (4H, m, β-methylene), 1.41 (10H, m, γ-, δ-, and α-methylene). ^{13}C NMR (75.5 MHz, TFA-*d*): δ 162.4 (carbonyl), 42.91 (α-methylene), 31.05 (ϵ-methylene), 30.96 (β-methylene), 30.37 (δ-methylene), 28.50 (γ-methylene). Furthermore, the characteristic signals found in the prepolymer and attributed to the terminal groups were not detected in the NMR spectra of the post-polymerized samples.

The infrared spectrum of nylon 9,2 shows characteristic amide and methylene absorption bands: 3304 (amide A), 3052 (amide B), 2922 and 2852 (C−H), 1652 (amide I), 1516 (amide II), 786 (amide V), 722 (C−H), and 536 cm^{-1} (amide VI). It should be pointed that the amide I band appears with a remarkable asymmetry (noted as a shoulder at 1684 cm^{-1}) and that the amide II, V, and VI bands appear at different frequencies than those usually observed in polyamides (i.e., 1550, 690, and 580 cm^{-1}, respectively for nylon 6[28]). Such shifts may be attributed to the unique structure of the oxamide group, with two neighbor amides as compared with those of isolated amide groups.[29] The absorptions

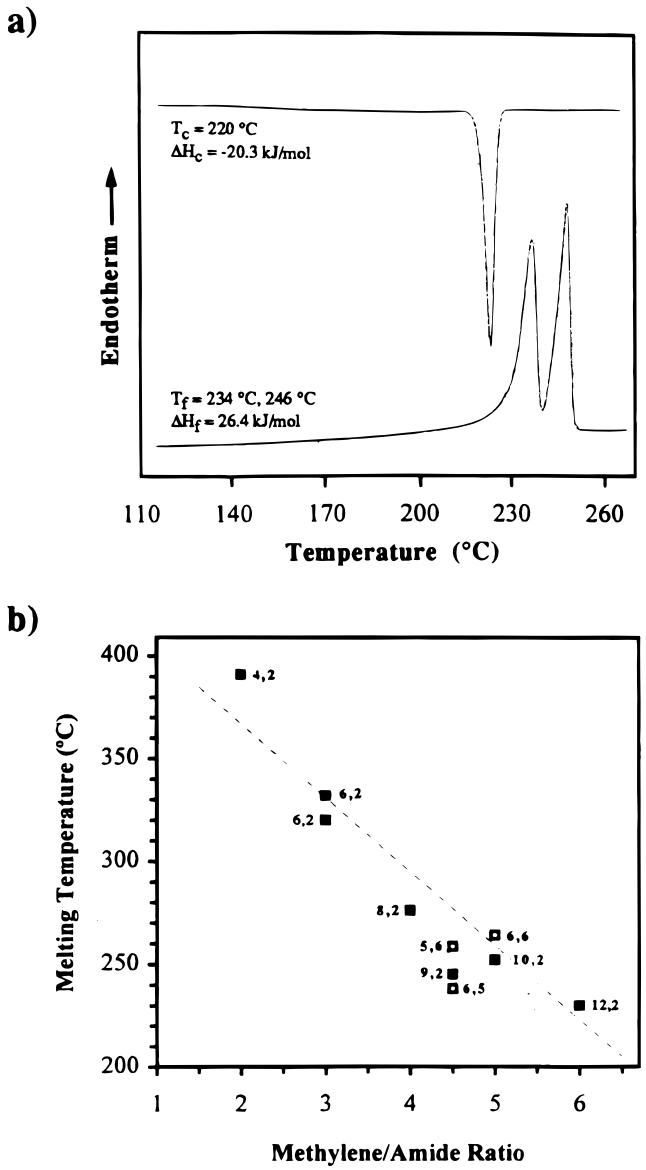

Figure 2. (a) Heating and cooling DSC traces for solution-crystallized samples of nylon 9,2. In both cases the rate was 20 °C/min. (b) Melting temperature vs the methylene/amide ratio of polyoxamides[10,14,15] (■). Note that two different temperatures appear in the literature for nylon 6,2. For comparison purposes selected nylons (□) are included in the representation: nylon 6,6,[33] nylon 5,6,[33] and nylon 6,5.[21,33] Note that nylon 9,2 shows a melting temperature lower than nylon 10,2 in a clear disagreement with the averaged plot for even polyoxamides, which is represented by the dashed line.

found in nylon 9,2 compare well with the reported data on the series of even polyoxamides,[10] where an increase in the amide A, B, I, and II frequencies was observed when the number of methylene groups in the diamine decreases. Thus, the observed values are intermediate from those found in nylons 10,2 (3302 (amide A), 3047 (amide B), 1650 (amide I) and 1512 cm^{-1} (amide II)) and 8,2 (3315 (amide A), 3060 (amide B), 1655 (amide I) and 1518 cm^{-1} (amide II)). Since such variations were interpreted as a consequence of a weakness in the hydrogen bond interactions in the polyoxamide series, we conclude that nylon 9,2 presents similar hydrogen bond characteristics than the related nylons 10,2 and 8,2.

DSC studies of nylon 9,2 (Figure 2a) showed a double melting point (234 and 246 °C) in the heating run of a

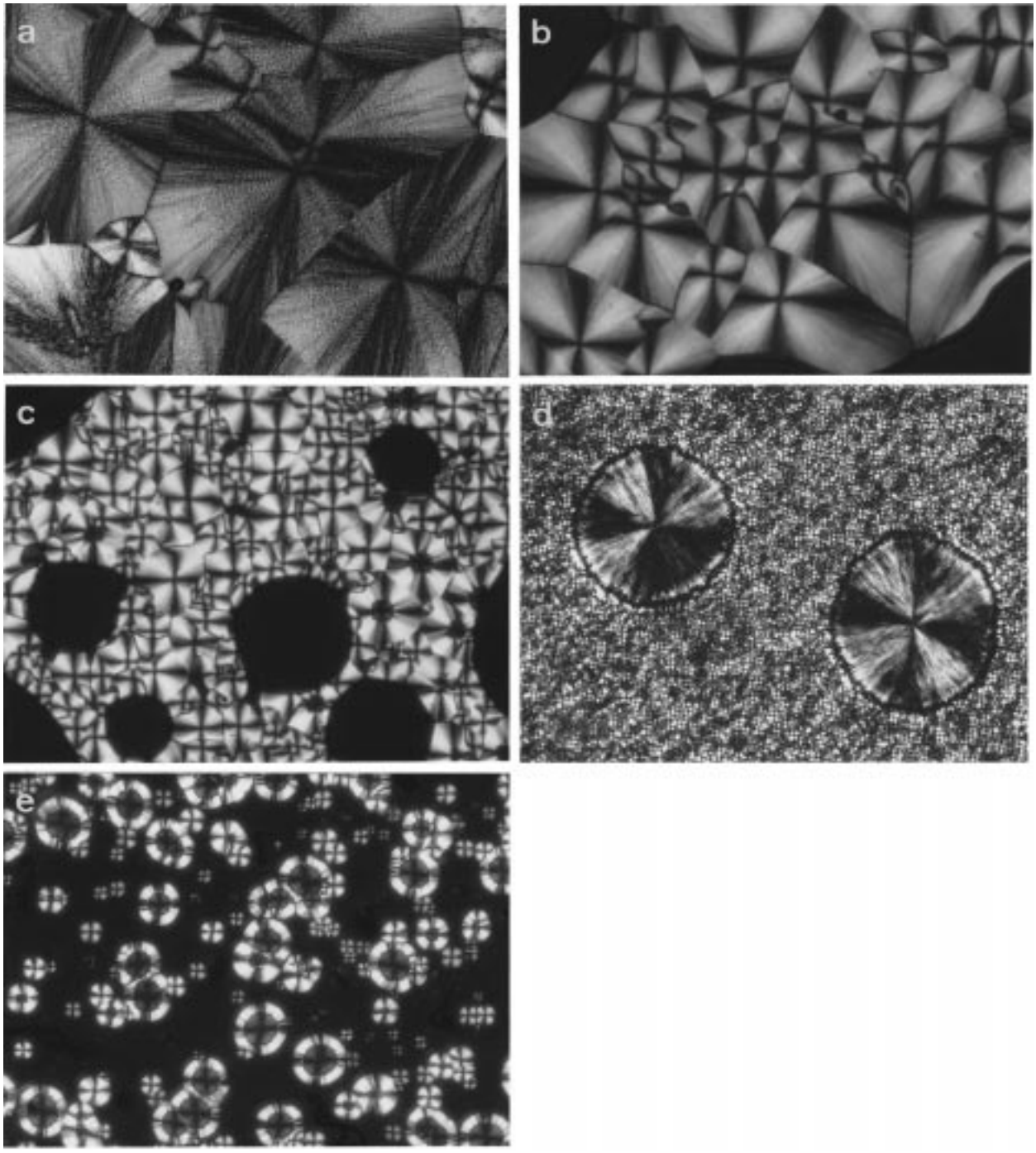

Figure 3. Photomicrographs of nylon 9,2 spherulites grown at different temperatures after fusion at 265 °C for 10 min: (a) ringed negative spherulites crystallized at 200 °C; (b) nonringed negative spherulite grown at 216 °C, where the spherulite displays a speckled appearance interpreted as an indication of incipient banding; (c) positive spherulites crystallized at 160 °C; (d) spherulitic aggregates formed at 238 °C, where small positive spherulites are also present in the grainy background; (e) nylon 9,2 complex spherulites grown by stepwise crystallization: negative spherulites initially grow at 193 °C (inner weakly birefringent region), subsequent crystallization at 140 °C renders a positive spherulite, which appears as a boundary ring with higher birefringence. Part a is given at 112× in order to see the rings in detail, while parts b, c, d, and e are given at 56× magnification.

solution-crystallized sample. This is a very common observation in thermal studies of nylons,[30] and it is usually interpreted as a recrystallization process on heating that affects the population of smaller crystallites whose melting point is lower. A high crystallinity (ca. 65%) could be deduced from the heat of fusion and an estimated value of 40 kJ/mol for a 100% crystalline sample.[31] The subsequent cooling run showed that the material crystallizes well (ca. 45%) from the melt, giving a single exotherm at 221 °C.

It should be noted that the melting temperature of nylon 9,2 is lower than the expected value derived from the reported data on even polyoxamides.[10,14,15] This fact is in agreement with thermal studies on nylons,[32] which indicate higher melting temperatures for even−even nylons than for odd−even and even−odd nylons with a similar methylene/amide ratio. Thus, Figure 2b shows that the melting temperatures of even polyoxamides regularly increase with the reduction of the methylene/amide ratio and also that the measured value for nylon

9,2 does not fit with the averaged linear plot. On the contrary, the melting temperature of nylon 9,2 is in close agreement with the reported data on odd−even and even−odd nylons with the same methylene/amide ratio (i.e., 258 °C for nylon 5,6[33] and 241 °C for nylon 6,5[21,33]). In the same way, even−even nylons have melting temperatures similar to those of even polyoxamides (i.e., 265 °C for nylon 6,6[33]).

Types of Spherulites. Examination of films prepared from the melt showed that at least three types of spherulites can be formed in nylon 9,2: (a) negative spherulites, both ringed (Figure 3a) and nonringed (Figure 3b), (b) positive spherulites (Figure 3c), and (c) spherulitic aggregates (Figure 3d). These diverse kinds of spherulites are usually formed in other nylons by direct crystallization from the melt as reported by Magill[34−38] and Lovinger.[39,40] The characterization of spherulites is based on the nature of their birefringence. It has been shown that within a positive spherulite the hydrogen-bonded sheets are parallel to the direction of growth (maximum birefringence index), whereas the negative spherulites proceed by radial stacking of hydrogen-bonded sheets.[40] In addition, spherulitic aggregates, which are highly birefringent but with confusing optical properties, have also been found.

The observed spherulitic texture and birefringence depends mainly on the growth temperature. Thus, the entire range of spherulitic structures can be obtained for nylon 9,2 within a single spherulite by controlled cooling during its crystallization from the molten stage (Figure 3e).

At crystallization temperatures of 192 °C and higher, up to the melting point, negative spherulites are the most prevalent kind encountered in the crystallization of nylon 9,2. Ringed negative spherulites clearly form over a fairly narrow temperature interval between 192 and 216 °C. The concentric extinction bands are indicative of lamellar twisting, which has been explained, in some cases, as a consequence of surface stresses derived from chain tilt in the crystals.[41] No measurable change in ring spacing was detected on raising the temperature although the magnitude of the birefringence increased (until 220 °C), probably due to some reorganization within the spherulite. Thus, samples melted at 265 °C and crystallized at 195, 200, 205, and 210 °C had an average spacing of 7 μm. It is impossible to resolve microscopically any discernible change in the spacing of the fine ringed portions beyond 210 °C, but ringed characteristics continue because spherulites at 216 °C display a speckled appearance interpreted as an indication of incipient banding. At temperatures close to the melting point (235−238.5 °C) spherulitic aggregates which are about two times larger than the ringed negative spherulites can be observed (Figure 1d). These aggregates have a homogeneous center of low positive birefringence with one discernible ringed overgrowth of higher positive birefringence (not readily observable in the black and white photograph). The grainy background, which consists of smaller positive spherulites, is the product of crystallization during cooling of the material still uncrystallized at the initial crystallization temperature.

At temperatures less than 192 °C approximately, positive birefringent spherulites, with the arms of the maltese cross parallel and perpendicular to the principal vibrations of the incident polarized light, are predominately formed.

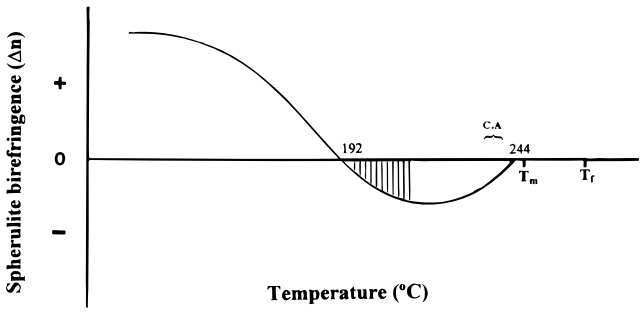

Figure 4. Schematic summary of spherulite formation in nylon 9,2. Birefringence in arbitrary units is represented as the ordinate with temperature as the abscissa. The hatched area indicates the region where ringed spherulites grow. T_f is the maximum melting temperature (265 °C) used in this work, and T_m represents the polymer melting point (246 °C). C.A. denotes crystalline aggregate.

The general pattern of spherulitic crystallization for nylon 92 is summarized in a schematic diagram (Figure 4). The ordinate in this figure is an arbitrary birefringence scale which serves to give the temperature range (abscissa) over which structures have been observed to grow.

Electron Microscopy. Different morphologies, depending on the crystallization temperature, were obtained from dilute solutions in 1,4-butanediol. Lamellar crystals begin to develop at temperatures near 75 °C and appear folded over themselves (Figure 5a). A uniform crystallization is achieved at 110 °C (Figure 5b), the individual lamellae (Figure 5c) have a lenticular shape (indicative of a lozenge habit) with dimensions close to 3 μm long and 0.7 μm width. These crystals appear to be flat, since no striation, indicative of pyramidal structures that collapse on sedimentation, has been detected. It should be pointed out that similar morphologies are observed for the orthorhombic structure of polyethylene, when crystallization is carried out at high temperatures. In this case the {100} growth face becomes rounded and predominates over the {110} faces (responsible of the lozenge shape). This characteristic curvature of the nominally {100} facets has recently had a major impact on kinetic theories of crystallization.[42,43]

Elongated multilayered lath-shaped crystals (Figure 5d) were obtained at a higher crystallization temperature (>120 °C). Note that in this case crystallization was less uniform and so crystals with a rather variable length were obtained. Note also that the lenticular appearance is also manifest in the smaller crystals. Two common characteristics were found in the reported crystallizations: (i) a lamellar thickness close to 50 Å (as estimated from their shadow in the micrographs) and (ii) the lamellae present rough growth faces. All these features are similar to those found in nylon 6,6.[45]

Electron diffraction patterns (Figure 6, parts a and b) were obtained from the lamellar crystals. All the reflections could be indexed (Table 1) assuming a monoclinic unit cell with parameters a = 5.45 Å, b = 8.7 Å, c (chain axis) = 31.8 Å, and β = 47.9°. Thus, the observed variability in the diffraction patterns may be interpreted as due to different degrees of tilting of the samples. The following features can be derived from the diffraction patterns: (a) An *mm* symmetry is apparent and so a triclinic structure can be rejected. (b) The most intense *hk*0 reflections correspond to the spacings of 4.34 and 3.65 Å (Figure 6a), which are

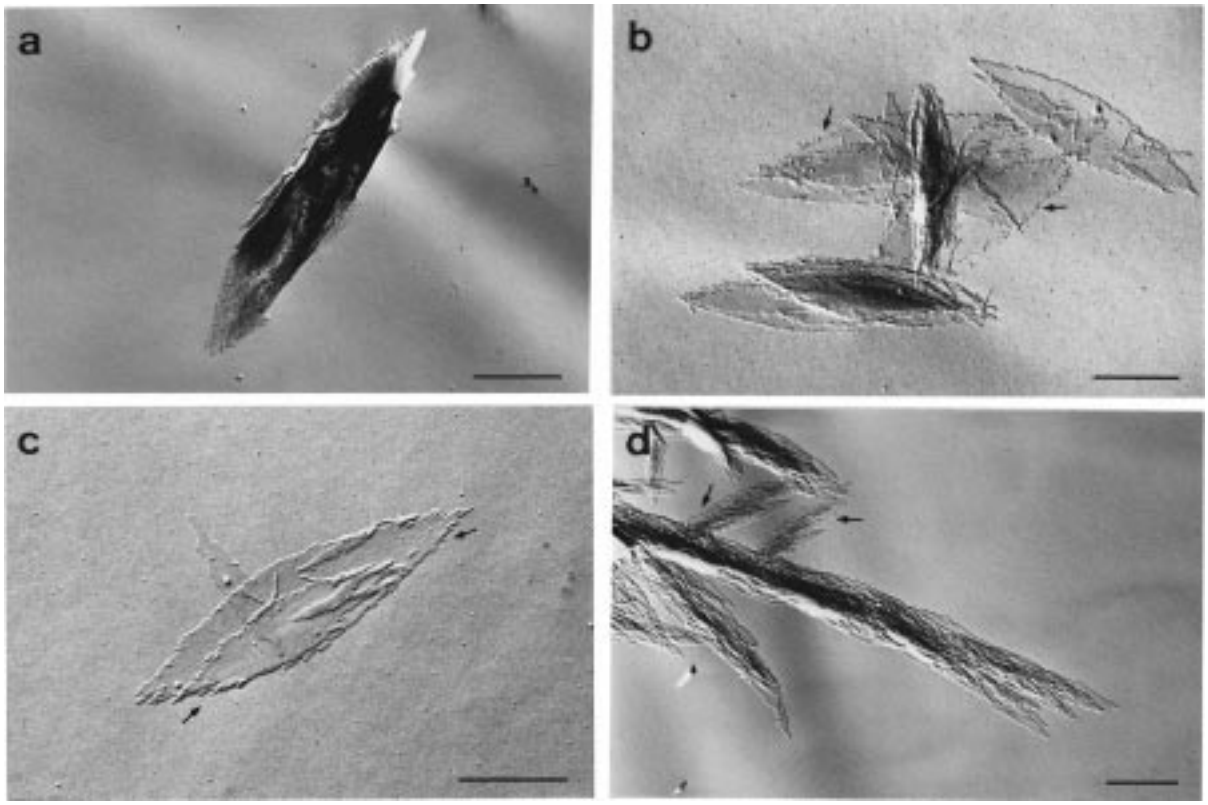

Figure 5. Transmission electron micrographs of nylon 9,2 obtained from 1,4-butanediol solutions at different crystallization temperatures: (a) 75 °C, (b and c) 110 °C, and (d) 120 °C. Note the serrated growth faces (see arrows) of the lenticular crystals depicted in parts b and c. These morphologies are still present (arrows) in the crystallization where elongated crystals predominate (d). Scale bar = 1 μm.

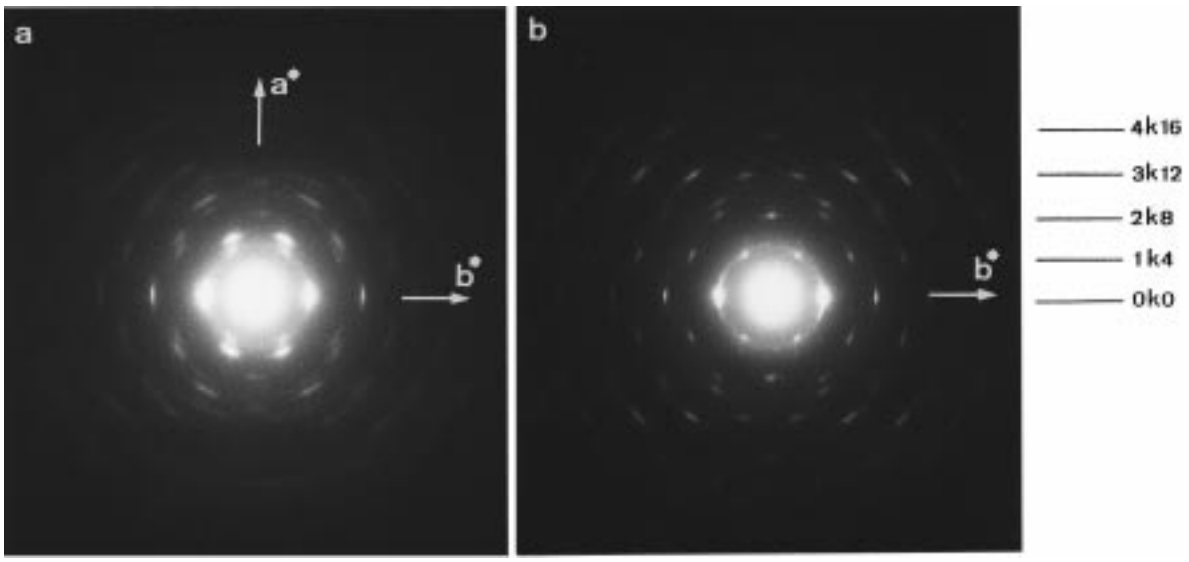

Figure 6. Selected area diffraction patterns of nylon 9,2: (a) sample tilted around the *b* axis; (b) untilted sample. The layer lines parallel to b* correspond to 1*k*4, 2*k*8, 3*k*12, ...reflections. Note in both cases the sharpeness of the 020 reflection and the symmetry of the patterns.

usually attributed to the α form of nylons. (c) In all patterns the 020 reflection (4.34 Å) is intense and appears to be oriented in the direction of the long axis of the crystals. On the contrary, the 110 reflection (3.65 Å) has a variable intensity as a function of the degree of tilting and is practically unobservable in the untilted samples (Figure 6b). These facts indicate that molecular chains are inclined with respect to the crystal basal plane in the *a* direction, in agreement with the β monoclinic angle. (d) The projection of the crystal structure along the chain axis direction gives a rectangular unit cell with parameters a_p = 4.04 Å and b_p = 8.7 Å. The diagonal length is 9.58 Å, which corresponds to twice the separation distance between hydrogen-bonded chains. An angle of 49.7° between both diagonals is also derived. These cell dimensions and the systematic absences in the diffraction patterns (*hk*0 with $h + k$ = odd) suggest a *C*-centered unit cell. (d) The 114 reflection appears with a medium intensity in the untilted patterns. This fact can be well explained by taking into account that the 114 planes are practically perpendicular to the 001 basal plane. In the same

Table 1. Measured and Calculated Electron Diffraction Spacings (Å) of Lamellar Crystals of Nylon 9,2

index[a]	calcd spacing	measd spacing	intensity[b]
020	4.35	4.34	vs, vs
040	2.17	2.17	m, m
060	1.45	1.45	w, w
080	1.085	1.085	vw, vw
110	3.67	3.65	s, vw
111	4.01	4.07	w, -
114	4.62	4.65	w, m
130	2.36	2.36	w, -
134	2.56	2.56	w, m
154	1.66	1.65	vw, w
174	1.21	1.21	vw, -
200	2.02	2.01	w, -
208	2.72	2.78	vw, m
220	1.83	1.82	vw, -
223	2.09	2.10	vw, m
225	2.22	2.21	m, vw
228	2.31	2.36	vw, m
243	1.61	1.61	, vw
245	1.67	1.67	w, vw
248	1.70	1.73	, vw
268	1.28	1.27	w, vw
288	1.01	1.02	-, vw
3,1,12	1.78	1.84	vw, w
3,3,12	1.54	1.59	vw, m
3,5,12	1.26	1.29	vw, m
3,7,12	1.03	1.04	vw, w
408	1.25	1.21	-, vw
4,0,16	1.36	1.42	-, w
4,4,16	1.16	1.19	-, w
4,6,16	0.99	1.02	-, w

[a] On the basis of a centered monoclinic unit cell with parameters: $a = 5.45$ Å, $b = 8.7$ Å, $c = 31.8$ Å, and $\beta = 47.9°$. [b] The intensity observed in both patterns of Figure 6 is reported. The data on the right correspond to the untilted sample (Figure 6b). Abbreviations: vs, very strong; s, strong; m, medium; w, weak; vw, very weak.

way the *hkl* planes with $l = 4h$ are also perpendicular, and so it is possible to interpret the moderate intensity of the 1*k*4, 2*k*8, 3*k*12, and 4*k*16 layer lines observed in the untilted patterns appears. (e) Up to four orders of the 4.34 Å basic spacing can be seen, indicating that the structure is well preserved up to 1 Å resolution.

From the lamellar thickness and the molecular weight of the polymer (samples with an intrinsic viscosity of 0.57 dL/g were employed in all crystallization experiments), we conclude that the molecular chains are folded within the lamellae. This thickness is compatible with four oxamide units in the straight stem of the lamellar core and a re-entry folding, which probably takes place through the polymethylenic segment of the diamine and presumably along the [110] and [110] directions (hydrogen-bonding directions, as will be discussed in the next sections).

Figure 7 shows the polyethylene decoration of nylon 9,2 crystals. Although polyethylene rods are hardly oriented on the lenticular crystals, some domains can be observed. Thus, the rods usually appear in an oblique disposition with respect to the curved growth faces. This orientation is in agreement with the fact that these surfaces are not strictly parallel to the hydrogen bonding direction where folding is assumed to take place. In the case of the elongated crystals depicted in Figure 7b, we see mainly a perpendicular orientation of the polyethylene rods with respect to the long axis of the crystals, but some crystals (upper right corner) show an oblique orientation

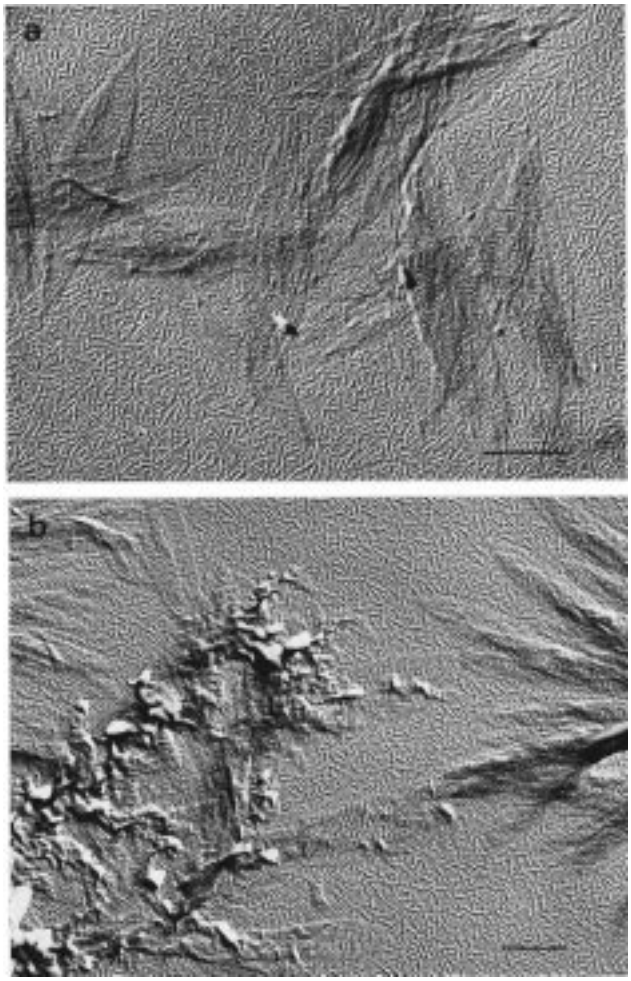

Figure 7. Crystals of nylon 9,2 decorated with polyethylene using the Wittmann and Lotz[43] technique and shadowed with Pt/C at an angle of 15°: (a) lenticular crystals obtained at 110 °C; (b) lath-shaped crystals obtained at 120 °C. Scale bar = 1 μm.

X-ray Diffraction. The X-ray diffraction patterns of samples obtained directly after post-polymerization (and so melt crystallized) are characterized by two intense rings in the wide angle zone. Whereas one of them always appears at the 4.34 Å spacing found in the electron diffraction patterns of single crystals, the other one has a rather variable spacing in the 3.90−3.67 Å range. However, when the sample is precipitated or crystallized from solution, the second ring appears around 3.67 Å, in close agreement with the electron diffraction data. Table 2 summarizes the main reflections observed in powder patterns of precipitated samples, mats of sedimented single crystals prepared from 1,4-butanediol solutions (Figure 8) and fibers annealed at 120 °C under stress (Figure 9). The measured spacings are similar within experimental error and can be indexed with the monoclinic unit cell derived from the electron diffraction pattern. Moreover the experimental density (1.15 g/cm^3) is in agreement with the calculated value (1.26 g/cm^3) for such unit cell, if we take into account the influence of the amorphous material. Additional considerations from the diffraction patterns are as follows:

(a) The most intense reflections (4.34 and 3.67 Å) are related to chain packing, since an equatorial orientation

Table 2. Measured and Calculated Diffraction Spacings for Different Nylon 9,2 Samples: Powder Recovered from Precipitation of Dichloroacetic Acid Solutions, Mat of Sedimented Crystals Obtained from 1,4-Butanediol Solutions, and Annealed Fiber

		measd spacings (Å)[b]		
index[a]	calcd spacings (Å)	powder	mat	fiber
lamellar thickness	49		49 vs M	
2nd order	24.5		24.5 w M	
4th order	12.25		12.24 vs M	
5th order	9.80		10.00 m M	
9th order	5.44		5.40 vw M	
002	11.80	11.76 vs		11.80 m off M
004	5.90	5.90 w		
113, 114	4.55, 4.62		4.65 vw	
020, 021, 112	4.35, 4.27, 4.33	4.35 vs	4.34 vs E	4.35 s E
111	4.01	4.02 w	4.05 w	
11$\bar{0}$	3.67	3.67 vs	3.68 vs off M	3.75 s E
11$\bar{1}$, 025	3.33, 3.20	3.27 vw	3.25 w	
11$\bar{2}$	3.02	2.98 vw	2.99 vw	
11$\bar{3}$	2.75		2.79 w	
11$\bar{4}$	2.51	2.55 vw	2.55 w	
11$\bar{5}$,131	2.30, 2.44	2.33 w	2.35 w	
11,13	2.26	2.30 vw	2.27 w M	
040, 22,12	2.17, 2.12	2.08 vw	2.12 w	

[a] On the basis of a centered monoclinic unit cell with parameters: $a = 5.45$ Å, $b = 8.7$ Å, $c = 31.8$ Å, and $\beta = 47.9°$. [b] Abbreviations denote intensities or orientation: vs, very strong; s, strong; m, medium; w, weak; vw, very weak; M, meridional; E, equatorial; off M, off-meridional.

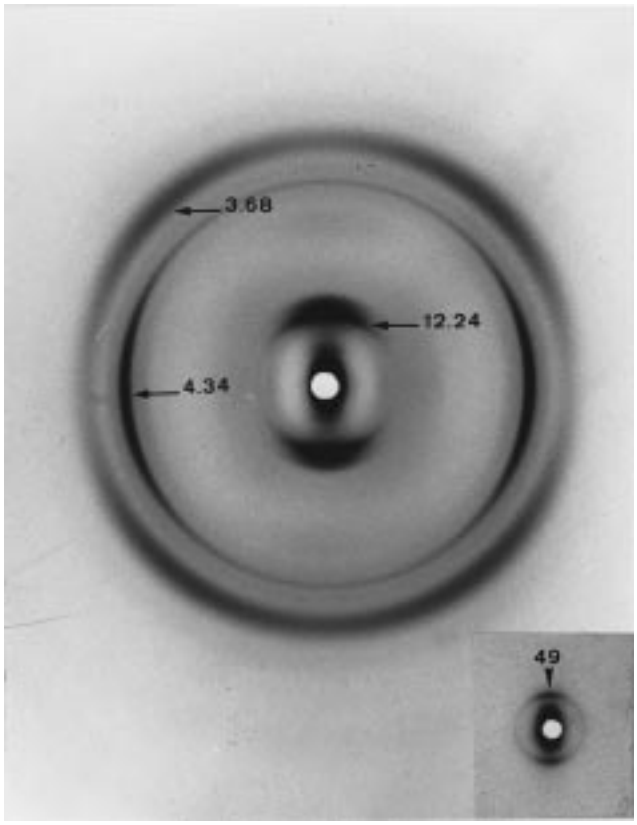

Figure 8. Wide-angle X-ray diffraction pattern obtained from a mat of sedimented crystals of nylon 9,2, with the main diffraction signals labeled. Crystals were prepared by isothermal crystallization at 120 °C of a dilute 1,4-butanediol solution. Note the angular splitting of the 110 reflection above and below the equator. Strong diffraction in the meridional region corresponds to two orders of the lamellar spacing, at 12.24 Å (indicated) and 10.0 Å. A meridional reflection (49 Å) related to the lamellar thickness is present in the low-angle pattern (inset).

is detected in the fiber patterns. These values are close to the characteristic diffraction signals of the α form of nylons[16] and also to the reported data for nylons 6,5[21]

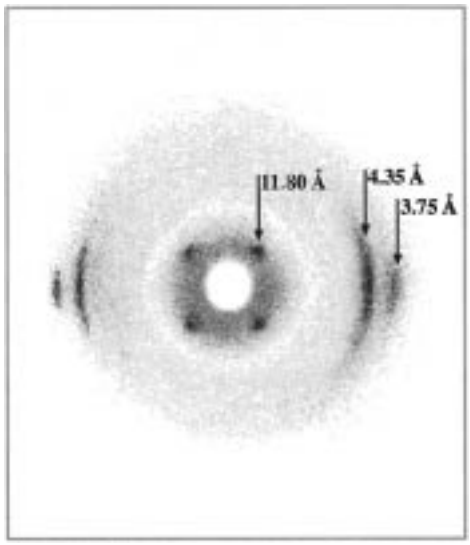

Figure 9. X-ray diffraction pattern of an oriented fiber of nylon 9,2. The 002 reflections appear at ca. 42° at either side of the meridian with a spacing of 11.8 Å.

and 12,5[23] where a new structure with two hydrogen bond directions has been postulated.

(b) A limited number of reflections were observed in the fiber pattern due to the very narrow fibers that could be obtained by melt extrusion. Fibers with larger diameters were disoriented because of spherulitic crystallization. However, direct evidences for the chain repeat length (15.9 Å) and the *cc** angle (ca. 42°) could be obtained from the 002 reflections. Note that the chain repeat is very close to the expected value (32 Å) for an all-trans conformation.

(c) An off-meridional orientation (ca. 45°) is observed for the very strong reflection at 3.68 Å spacing in the mat diffraction pattern, whereas the 4.34 Å spacing appears in the equator. This fact together with the meridional orientation of the lamellar spacings indicates that the crystals are sedimented on the 00*l* planes and confirms that the monoclinic angle corresponds to β.

(d) A lamellar thickness of 49 Å can be derived from the low and wide-angle diffraction patterns of sedimented crystals. It should be pointed that the 4th, 5th, and 9th lamellar orders, which are close to the 00*l* reflections, appear intensified. Moreover, the fact that so many orders are observed indicates that the lamellar thickness is fairly constant and that neighboring lamellae in the stacking diffract coherently, as happens in other nylons.[46] However, some additional weak reflections (17.55 and 14.88 Å) can be seen in the low angle region and constitute a puzzling feature. Thus, they cannot be indexed as lamellar orders, since a thickness higher than 100 Å should be required in disagreement with the electron microscopy measurements. The reduced number of chain repeat units in the lamellar thickness may contribute to these reflections.

Structural Modeling. Although both the intense interchain diffraction signals at ca. 4.34 and 3.67 Å, and the chain repeat length are close to the expected values for an α form, this structure appears highly unlikely due to the unsatisfactory hydrogen bond geometry, as illustrated in Figure 1. Note that all hydrogen bonds cannot simultaneously be established in a single plane when the conformation is all-trans. However, slight distortions on the torsion angles may produce a rotation between consecutive oxamide planes, and consequently hydrogen bonds along two directions can be satisfied when neighboring chains are conveniently shifted. Similar structures have recently been reported for even−odd nylons as those derived from malonic[20] and glutaric acid[21,23] and also[47] in nylon 6,9. In this case, the rotation between amide planes seems to be additionally favored by a repulsive electronic interaction between the close carbonyl groups of the diacid moiety. The *mm* symmetry found in the electron diffraction patterns of nylon 9,2 is an additional indication of this new structure. If a single hydrogen bond direction was present, the oxamide planes should be aligned along the monoclinic unique axis *b*, in order to comply with symmetry requirements, but the experimental value of the *b* parameter does not fit at all with the expected value for hydrogen-bonded chains (8.7 vs 4.79 Å, respectively).

Different models were built with the CERIUS 3.1 program, using standard bond distances and bond angles. Furthermore, all the X-CH_2−CH_2−Y torsion angles were kept in the trans conformation, as well as the three torsion angles (−NH−CO−CO−NH−) of the oxamide unit, in agreement with the model compounds found in the Cambridge Structural Data Base.[48] Thus, only the φ_1 and φ_2 torsion angles, which correspond to the two −CH_2−NH− dihedrals of the same residue, were refined. A molecular symmetry characterized by both, (i) a binary axis perpendicular to the chain direction through the central carbon of the diamine unit ($\varphi_1 = \varphi_2$) and (ii) a center of symmetry in the middle of the oxamide group appear compatible with the unit cell parameters and a $C12/c1$ space group. This symmetry has the consequence that equivalent torsion angles of consecutive repeat units are equal, but with opposite signs. Note also that when φ_1 deviates from 180°, the oxamide planar groups rotate from the plane defined by the polymethylenic zigzag. Thus, a rotation angle τ may be defined between the two C−O directions of the −$CONH(CH_2)_9NHCO$− segments. Note also (Figure 10) that small deviations of φ_1 with respect to the trans conformation ($\varphi_1 = 155°$) result in a significant rotation

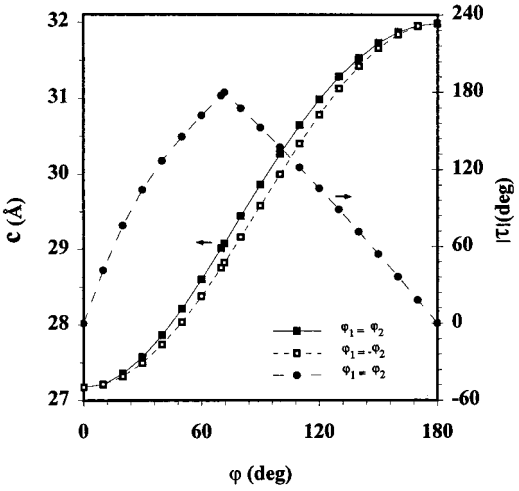

Figure 10. Calculated chain repeat lengths and absolute values of the rotation angle between consecutive oxamide units for different φ_1 torsion angles (φ_1 is the torsion of the nitrogen-methylene bond). Both $2_1/m$ and $2/c$ molecular symmetries are considered. In the case of $\varphi_1 = -\varphi_2$, the rotation angle τ is always equal to 0°.

angle ($\tau = 45°$), which is very close to that found between the two diagonals of the unit cell (49.7°) projected onto a plane perpendicular to the chain axis. Furthermore, a chain repeat length of 31.8 Å (equal to the experimental value) is obtained for the indicated conformation ($\varphi_1 = 155°$ and $2/c$ as a molecular symmetry).

These results are also in agreement with recent quantum mechanical calculations,[49] which predict a value of 163° for the torsion angle −NH−CH_2− of nylon 6,6. Furthermore, X-ray diffraction data indicate a deviation of the oxygen atoms from the plane defined by the methylene carbons.[50] Note that when $\varphi_1 = -\varphi_2$, both amide groups are contained in the same plane ($\tau = 0°$ or 180° depending on the even or odd number of methylene carbons between them), and so a structure with a single hydrogen bond direction is obtained (α or γ forms, according to the value of φ_1). On the contrary, $\varphi_1 = \varphi_2$ produces a rotation in opposite sense of the two amide planes and so gives a structure with two hydrogen bond directions. Figure 11 shows a projection down the chain axis of the proposed nylon 9,2 structure. Each molecule is hydrogen-bonded to its four neighbors and each oxamide unit rotates 22.5° from the plane of the methylene groups. Lateral projections of this structure are depicted in Figure 12. A shift between the hydrogen bonded chains gives a standard geometry ($d_{H\cdots O} = 2.05$ Å and $\angle NHO = 176.8°$) and justifies the β monoclinic angle. Moreover, the experimental value of 47.9° just corresponds to the displacement that optimizes this hydrogen bond geometry. Note also that the non-hydrogen-bonded chains are separated by a distance of 4.04 Å and that these molecules are shifted three bonds along the chain axis direction, in a similar way to the α form of nylons[16]

Figure 13 shows the simulated X-ray fiber diffraction pattern, which is in good agreement with the experimental one. Thus, 002 corresponds to the most intense off-meridional reflection, and a weak signal at 4.01 Å appears between the very intense equatorial signals at 4.35 and 3.67 Å. Furthermore, the latter is the most intense reflection, and so it may be detected in the electron diffraction patterns of slightly tilted samples.

Finally, it should be pointed that a γ structure is

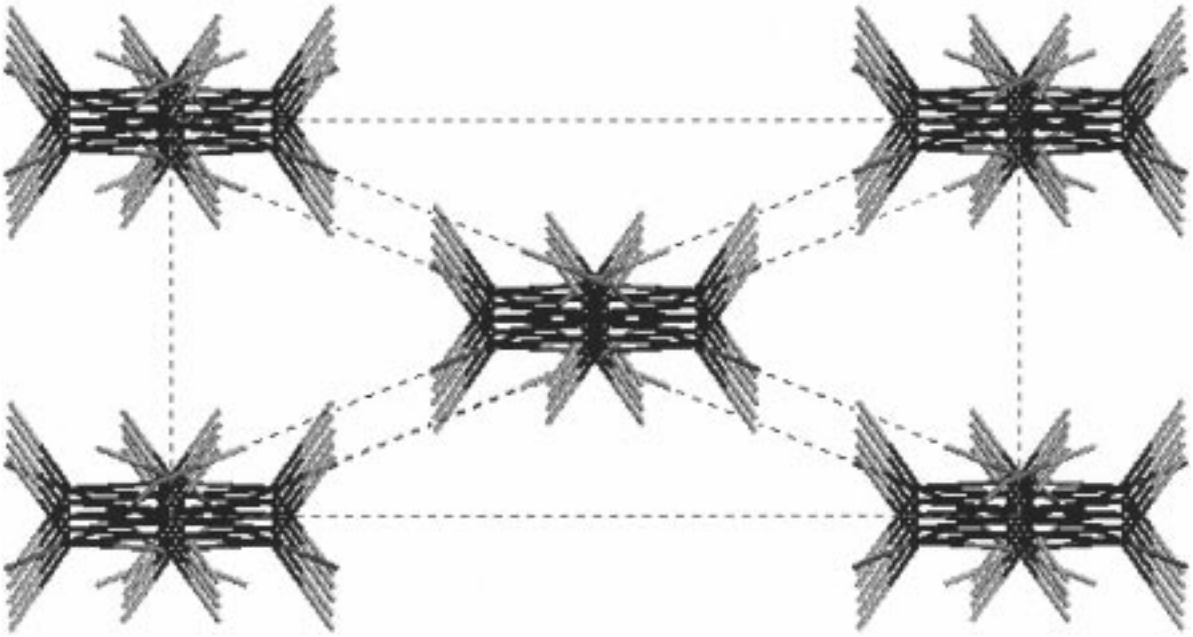

Figure 11. Equatorial projection of the centered unit cell. Note that hydrogen bonds (indicated by dashed lines) are established along both diagonals of the unit cell.

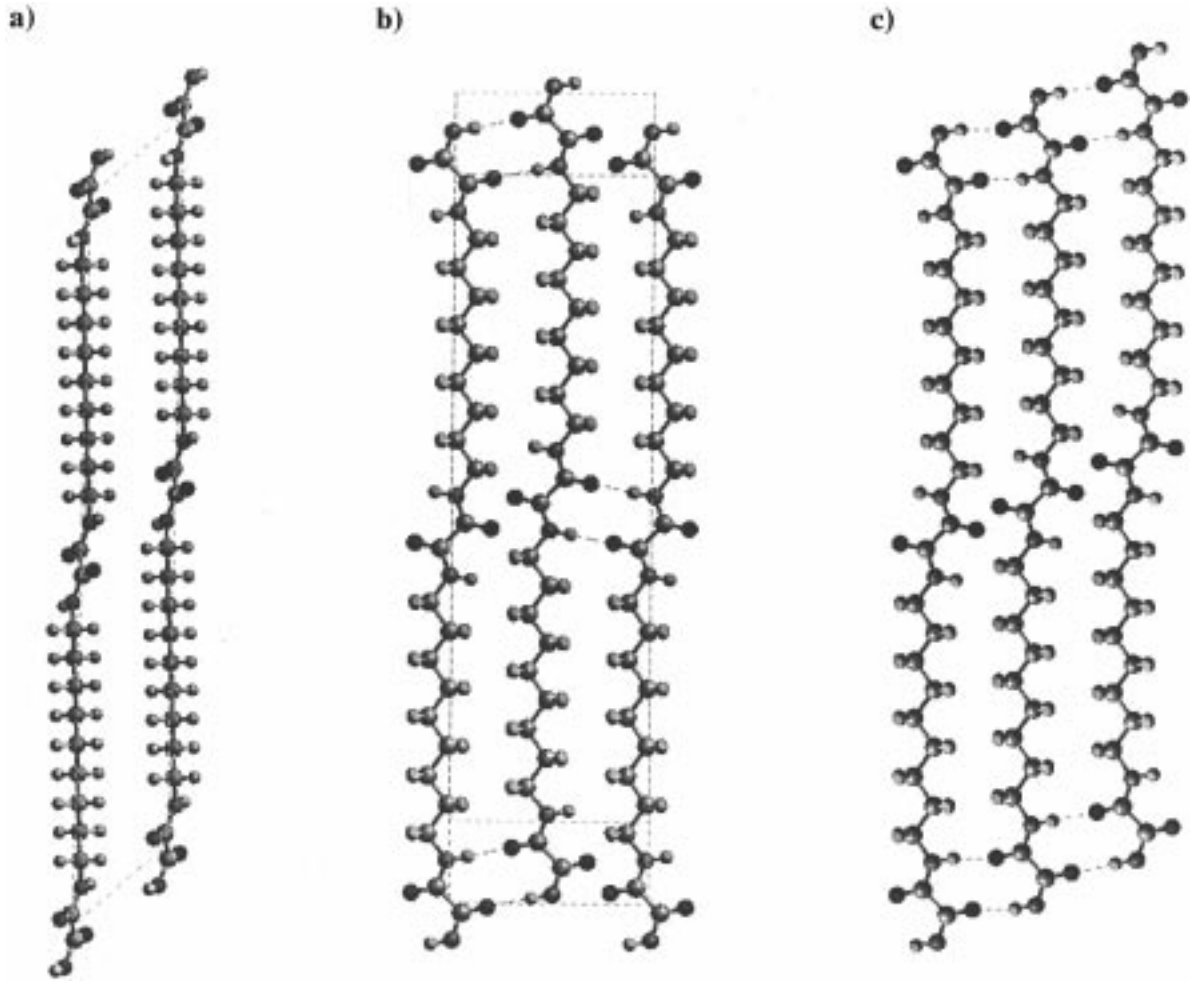

Figure 12. Different views of the nylon 9,2 structure. (a) *ac* projection of the unit cell, in this case a glide plane parallel to *ac* is manifest. Note that the neighboring chains are shifted approximately three bonds. (b) *bc* projection of the unit cell. The central molecular chain is at a different level in the *a* direction. (c) Three hydrogen bonded chains along the [110] direction. Note that the chains are shifted in order to optimize the hydrogen bonding geometry.

usually postulated for even−odd and odd−even nylons in order to optimize the hydrogen bond interactions. However, there are some considerations that make this structure unlikely for nylon 9,2:

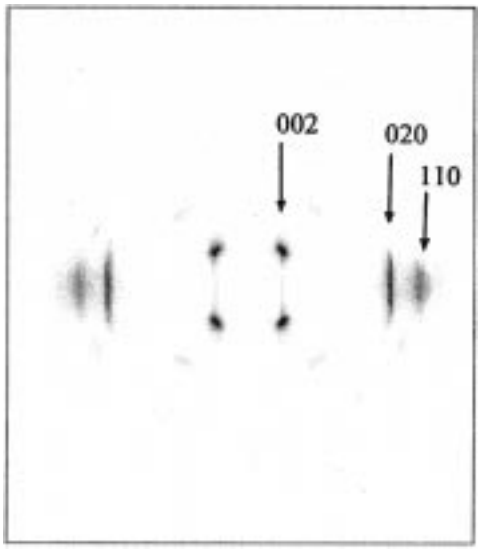

Figure 13. Simulated X-ray fiber diffraction pattern obtained with the CERIUS program and using an isotropic temperature factor $\exp[-B((\sin\theta)/\lambda^2)]$ with $B = 10$ A^2.

(a) The chain repeat length for $\varphi_1 = -\varphi_2 = 120°$ should be 30.8 Å (Figure 10), which is very far from the experimental value.

(b) In disagreement with the pseudohexagonal γ form of Kinoshita,[51] c and c^* are not coincident.

(c) The $2_1/m$ molecular symmetry expected for a γ form does not explain the mm symmetry found in the electron diffraction patterns of lamellar crystals.

Crystallization from the melt gives basically two types of spherulites (positive and negative), which in nylons with a single hydrogen bond direction have been explained according to the different disposition of hydrogen bonds with respect to the spherulitic radius. This explanation cannot be applied if the new structure is taken into account. However, although hydrogen bonds are established in two different directions, they form an angle of ca. 50 or ca. 130° depending on the direction along which we look at the structure (*b* axis or *a* axis, respectively). In our opinion this asymmetry may also explain the different spherulitic growth.

Brill Transition. Diffraction studies of nylons during heating show that the two basic spacings, which are related to chain packing, tend to merge into a single one in the so-called "Brill" transition temperature. The results depend on the preparation[18] and thermal history[52] of samples as well as the type of nylon. Thus, the reported Brill temperature for nylon 6,6 (170−230 °C)[52−56] is well below its melting temperature (265 °C) as in other even−even nylons such as those derived from ethylenediamine.[57] A Brill temperature just prior to melting was found in other cases such as nylons 4,8, 4,10, 4,12, 6,12, 6,18, and 8,12,[58] and finally some polymers (i.e. nylon 6[59]) melt before they reach the Brill temperature. A complete understanding of this behavior does not yet exist, and so different hypotheses have been given. They vary from the development of a three-dimensional network of hydrogen bonds[18,47,60,61] to a transition that involves a mobility of methylene groups while hydrogen bonds remain unchanged and so arranged in a single direction.[21,54,62]

Changes with temperature in the spacings of the strong diffraction signals were monitored using X-ray patterns of sedimented crystal mats. Figure 14a shows the changes in the spacings of the two strong reflections

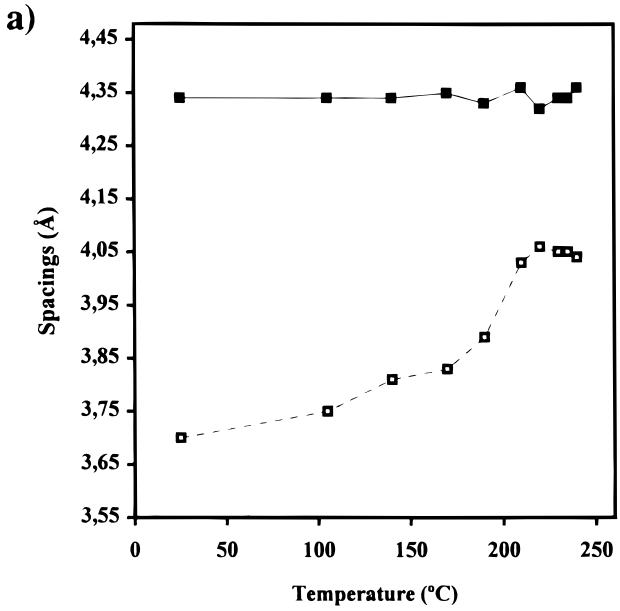

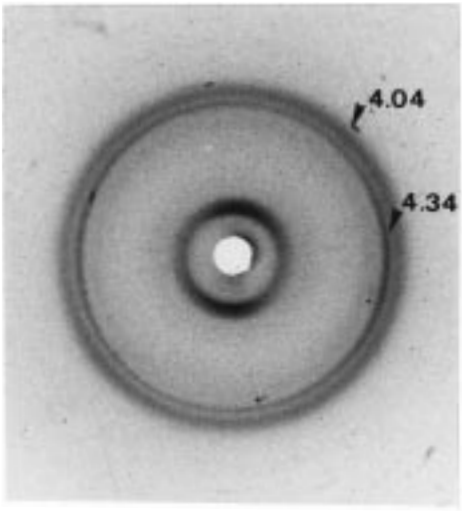

Figure 14. (a) Graph showing the change of the 020 (■) and 110/110 (□) spacings as nylon 9,2 mats are heated from room temperature to 245 °C. (b) Wide-angle X-ray diffraction pattern recorded at 240 °C from a mat of sedimented crystals.

(020 and 110/110), which at room temperature appear at 4.34 and 3.68 Å. While the spacing of the first diffraction signal remains practically constant, the second one increases with temperature until a maximum spacing of ca. 4.05 Å, reached at 215 °C (ca. 30 °C before melting). Figure 14b shows the high-temperature X-ray diffraction pattern of nylon 9,2 where the two interplanar spacings are still evident.

Thus a Brill transition in which both equatorial spacings merge into a single reflection has not been observed in this case. It should be noted that the breaking of an oxamide interaction between neighboring molecular chains must be very difficult for nylon 9,2, since two hydrogen bonds are involved in this case. Unfortunately we have been unable to collect additional reflections, so that it is not possible to obtain a tentative unit cell. Nevertheless, from the two reflections shown in Figure 14, it is possible to derive an equatorial projection, as given below in Table 3. We think that the observed change on lattice parameters with temperature is mainly caused by an enhanced mobility of

Table 3. Comparison of Rectangular Cell Bases[a] of Different Nylons Projected on a Plane Perpendicular to the Fiber Axis

nylon	a_p	b_p	ref
6,6	4.03	8.73	50
6,6 (200 °C)	4.85	8.40	55
9,2	4.04	8.70	this paper
9,2 (240 °C)	4.56	8.68	this paper
6,3	4.62	8.46	20
5,3	4.62	8.47	20
6,5	4.20	8.62	21
12,5	4.11	8.72	23

[a] The cell bases are centered and contain two molecules. Hydrogen bonds are oriented along one diagonal in nylon 6,6 and along both diagonals in the other cases.

methylenes, as demonstrated by Wendolowsky *et al.*[63] for nylon 6,6. Thus the system of two hydrogen bond directions is unchanged, and only the rotation angle between consecutive oxamide units varies slighlty, as has been postulated for nylon 6,5.[21]

Finally it should be pointed that the diffraction pattern shows spacings at 4.34 and 3.85 Å when the sample is cooled again to room temperature. Thus, the second reflection appears at slightly different spacings from the original crystallized sample. This observation is in agreement with the observed variability of the powder patterns of samples coming from the melt state (post-polymerization).

Comparison with Other Polyamides. The dimensions of the projected rectangular cell found for nylon 9,2, shown in Figure 11, are strikingly similar to those of nylon 6,6, as indicated by the dimensions given in Table 3. This is not surprising, since the structural organization of the parallel polymer chains is related in both structures, as is apparent from Figure 12. The main difference is that nylon 9,2 has hydrogen bonds along both diagonals of the projected rectangular cell, whereas nylon 6,6 has hydrogen bonds only along one diagonal. A consequence of such organization is that in the monoclinic cell of nylon 9,2, the central molecule in Figure 11 is placed at a height exactly intermediate between the lower and upper row of molecules. In the equivalent cell of nylon 6,6 the vertical displacement of the central molecule is different in the direction of the two diagonals.

Upon heating, nylon 9,2 does not undergo a Brill transition, although the unit cell dimensions change as shown in Table 3 and in Figure 14. The two rings in Figure 14b are clearly different. It is obvious that in this case the unit cell changes and the results obtained cannot be interpreted as the coexistence of a low and a high-temperature structure, as suggested[54] for nylon 6,6.

The values given in Table 3 also show that the mutual arrangement of the polymer chains is slightly different from that found in *n*,3 and *n*,5 polyamides, which also have two directions of hydrogen bonding and a projected cell similar to that shown in Figure 11. The different conformational angles due to the unique features of malonamide[20] and also the particular conformation of the even diamine subunits[20,21,23] may be the main reason for the observed deviations.

Conclusion

We have found that nylon 9,2 has a particular structure characterized by two hydrogen bond directions. From a conformational point of view, this structure is close to the characteristic α form of nylons. The main difference consists of the different rotation of consecutive amide groups along the polymer chain from the plane defined by the methylene carbons. In the α form of nylon 6,6 all the amide groups deviate in the same sense ($\varphi_1 = -\varphi_2$), giving a structure with a single hydrogen bond direction. In nylon 9,2 these consecutive amide planes deviate in opposite senses, and consequently they point into two different directions. Diffraction spacings are similar for both structures and clearly differ from those expected for a γ structure.

The proposed conformation ($\varphi_1 = \varphi_2$) is also possible in other odd−even and even−odd nylons, since it allows the establishment of all possible hydrogen bonds. The new structure is an alternative to the γ form commonly postulated for this type of nylons.

Acknowledgment. This research has been supported by research grants from CICYT (MAT97-1013) and DGICYT (PB93-1067). L.F. acknowledges financial support from the Ministerio de Educación y Cultura. We are also thankful to J. L. Marcos for his help in experimental manipulations.

References and Notes

(1) Ellingboe, E. K. U.S. Pat. (to E. I. DuPont de Nemours and Co.), 2,9, 37,161, 1960.
(2) Bruck, S. D. U.S. Pat. (to E. I. DuPont de Nemours and Co.), 2,9 77,340, 1960.
(3) Stamatoff, G. S.; et al. U.S. Pat. (to E. I. DuPont de Nemours and Co.), 3,2 47,168, 1966.
(4) Mileo, J. C.; et al., Ger. Offen. 1, 900,719, 1969; *Chem. Abstr.* **1969**, *71*, 125435*t*.
(5) Bruck, S. D. *Ind. Eng. Chem., Prod. Res. Dev.* **1963**, *2*, 119.
(6) Allen, S. J.; et al. U.S. Pat. (to Celanese Corp.), 2,558,031, 1951.
(7) Zimmerman, J.; U.S. Pat. (to E. I. DuPont de Nemours and Co.), 3, 432,575, 1969.
(8) Schlack, P.; Ger. Pat. (to Farbwerke Hoechst) 1,017,782, 1957; *Chem. Abstr.*, **1960**, *54*, 4056*d*.
(9) Black, W. B.; Preston, J. In *Man made Fibers-Science and Technology*; Mark, H. F., Atlas, S. M., Cernia, E., Eds.; Interscience: New York, 1968; Vol. 2, p 417.
(10) Shalaby, S. W.; Pearce, E. M.; Fredericks, R. J.; Turi, E. A. *J. Polym. Sci., Polym. Phys. Ed.*, **1973**, *11*, 1.
(11) Tirrell, D.; Vogl, O. *J. Polym. Sci., Polym. Chem. Ed.* **1977**, *15*, 1889.
(12) Muroi, S. *J. Appl. Polym. Sci.* **1966**, *10*, 713.
(13) Vogl, O.; Knight, A. C. *Macromolecules* **1968**, *1*, 315.
(14) Chatani, Y.; Ueda, Y.; Tadokoro, H.; Deits, W.; Vogl, O. *Macromolecules* **1978**, *11*, 636.
(15) Gaymans, R. J.; Venkatraman, V. S.; Schuijer, S. *J. Polym. Sci., Polym. Chem. Ed.* **1984**, *22*, 1373.
(16) Xenopoulos, A.; Clark, E. S. In *Nylon Plastics Handbook*, Kohan, M. I., Ed.; Hanser Publishers: Munich, Germany, 1995; Chapter 5.
(17) Kinoshita, Y. *Makromol. Chem.* **1959**, *33*, 1.
(18) Atkins, E. D. T.; Hill, M. J.; Veluraja, K. *Polymer* **1995**, *36*, 35.
(19) Vogelson, D. C. *J. Polym. Sci., Part A* **1963**, *1*, 1055.
(20) Puiggalí, J.; Aceituno, J. E.; Navarro, E.; Campos, J. L.; Subirana, J. A. *Macromolecules* **1996**, *29*, 8170.
(21) Navarro, E.; Franco, L.; Subirana, J. A.; Puiggalí, J. *Macromolecules* **1995**, *28*, 8742.
(22) Navarro, E.; Alemán, C.; Subirana, J. A.; Puiggalí, J. *Macromolecules* **1996**, *29*, 5406.
(23) Navarro, E.; Subirana, J. A.; Puiggalí, J. *Polymer* **1997**, *38*, 3429.
(24) Tereshko, V.; Navarro, E.; Puiggalí, J.; Subirana, J. A. *Macromolecules* **1993**, *26*, 7024.
(25) Navarro, E.; Puiggalí, J.; Subirana, J. A. *Macromol. Chem. Phys.* **1995**, *196*, 2361.
(26) Navarro, E.; Alemán, C.; Puiggalí, J. *J. Am. Chem. Soc.* **1995**, *117*, 7307.
(27) Pletcher, T. C.; Morgan, P. W. *J. Polym. Sci., Polym. Chem. Ed.* **1980**, *18*, 643.
(28) Abu-Isa, I. *J. Polym. Sci. A-1* **1971**, *9*, 199.

(29) Cannon, C. G. *Spectrochim. Acta* **1960**, *16*, 302.
(30) Wunderlich, B. *Macromolecular Physics*; Academic Press: New York, 1973.
(31) Van Krevelen, D. W. *Properties of Polymers*, 3rd ed.; Elsevier: Amsterdam, 1990.
(32) Champetier, G.; Monnerie, L. *Química macromolecular;* Espasa-Calpe: Madrid, 1973.
(33) Miller, R. L. In *Polymer Handbook*, 3rd ed.; Brandrup, J., Immergut, E. H. Eds.; Wiley-Interscience: New York, 1989.
(34) Magill, J. H. *J. Polym. Sci., Part A* **1965**, *3*, 1195.
(35) Magill, J. H. *Polymer* **1965**, *6*, 367.
(36) Magill, J. H. *J. Polym. Sci., Part A-2* **1966**, *4*, 243.
(37) Magill, J. H. *J. Polym. Sci., Part A-2* **1969**, *4*, 123.
(38) Magill, J. H. *J. Polym. Sci., Part A-2* **1971**, *9*, 815.
(39) Lovinger, A. J. *J. Appl. Phys.* **1978**, *49*, 5003.
(40) Lovinger, A. J. *J. Appl. Phys.* **1978**, *49*, 5014.
(41) Lotz, B. In Crystallization of polymers; Dosière, M., Ed.; Kluwer Academic Publishers: London, 1992; pp 17−23.
(42) Hoffman, J. D.; Miller, R. I. *Macromolecules* **1989**, *22*, 3038.
(43) Tanzawa, Y.; Toda, A. *Polymer* **1996**, *37*, 1621.
(44) Wittman, J. C.; Lotz, B. *J. Polym. Sci., Polym. Lett. Ed.* **1985**, *23*, 200.
(45) Hinrichsen, G. *Makrom. Chem.* **1973**, *166*, 291.
(46) Subirana, J. A.; Aceituno, J. E. *Macromol. Symp.* **1996**, *102*, 317.
(47) Franco, L.; Cooper, S. J.; Atkins, E. D. T.; Hill, M. J.; Jones, N. A. *J. Polym. Sci., Polym. Phys.* **1998**, *36*, 1153.
(48) Allen, F. H.; Kennard, O.; Taylor, R. *Acc. Chem. Res.* **1986**, *16*, 146.
(49) Dasgupta, S.; Hammond, W. B.; Goddard, W. A., III. *J. Am. Chem. Soc.* **1996**, *118*, 12291.
(50) Bunn, C. W.; Garner, E. V. *Proc. R. Soc. London A* **1947**, *189*, 39.
(51) Kinoshita, Y. *Makromol. Chem.* **1959**, *33*, 1.
(52) Ramesh, C.; Keller, A.; Eltink, S. J. E. A. *Polymer* **1994**, *35*, 2483.
(53) Brill, R. *Z. Phys. Chem.* **1943**, *1353*, 61.
(54) Hirschinger, J.; Miura, H.; Gardner, K. H.; English, A. D. *Macromolecules* **1990**, *23*, 2153.
(55) Murthy, N. S.; Curran, S. A.; Aharoni, S. M.; Minor, H. *Macromolecules* **1991**, *24*, 3215.
(56) Jones, N. A.; Atkins, E. D. T.; Hill, M. J.; Cooper, S. J.; Franco, L.; *Macromolecules* **1996**, *29*, 6011.
(57) Jones, N. A.; Cooper, S. J.; Atkins, E. D. T.; Hill, M. J.; Franco, L. *J. Polym. Sci., Polym. Phys. Ed.* **1997**, *35*, 675.
(58) Jones, N. A.; Atkins, E. D. T.; Hill, M. J.; Cooper, S. J.; Franco, L. *Polymer* **1997**, *38*, 2689.
(59) Radush, H. J.; Stolp, M.; Androsch, R. *Polymer* **1994**, *35*, 3568.
(60) Atkins, E. D. T.; Presented at Macromolecules'92: Functional Polymers and Biopolymers, Canterbury, U.K., Sept. 1992; Abstracts, p 10.
(61) Atkins, E. D. T. *Macromol. Rep.* **1994**, *A31* (Suppls. 6 & 70), 691.
(62) Colclough, M. L.; Baker, R. *J. Mater. Sci.* **1978**, *13*, 2531.
(63) Wendolowski, J. J.; Gardner, K. H.; Hirschinger, J.; Miura, H.; English, A. B. *Science* **1990**, *247*, 431.

MA971599Z